Theory of potential modulation in lateral surface superlattices

John H. Davies and Ivan A. Larkin
Department of Electronics and Electrical Engineering, Glasgow University, Glasgow G12 8QQ, United Kingdom
(Received 9 September 1993)

We have calculated analytically the potential generated in a two-dimensional electron gas by a lateral superlattice on a GaAs/$Al_xGa_{1-x}As$ heterostructure, formed by an array of parallel metal striped gates on the surface. The shape of the electrostatic potential produced by a bias on the gates depends on the boundary condition on the exposed surface of GaAs in the gaps between the gates. The usual assumption of a pinned GaAs surface gives a potential containing only odd harmonics. This is not in agreement with a recent experimental measurement of the potential from commensurability oscillations in the magnetoresistance. An alternative model where the surface charge is frozen in the gaps gives an asymmetry between the gates and the gaps which is closer to experiment. A quite different origin of the potential is a result of elastic strain resulting from differential contraction between the metal gates and the GaAs as the sample is cooled, coupling through the deformation potential. This gives a good fit to experiment and shows that the strain from mismatched gates cannot be neglected in electronic transport phenomena that are sensitive to weak potentials.

I. INTRODUCTION

The rapid growth of interest in ultrasmall semiconducting devices, particularly those based on a two-dimensional electron gas (2DEG), places ever-increasing demands on modeling. Electrons are guided by electrostatic potentials through structures analogous to electromagnetic waveguides, usually generated by applying a bias to patterned metal gates on the surface. One of the simplest structures is a pair of long parallel gates with a gap between, which produces a quantum wire or electron waveguide;[1,2] a short wire or quantum point contact shows the discrete nature of the transverse wave function directly through the quantized conductance.[3,4] Typical dimensions are around 0.1 μm, so even small voltages on the gates produce very high electric fields in the structure.

Although simulations of simple devices such as quantum point contacts give moderate agreement with experiment,[5] many basic features needed to model these structures are poorly understood. For example, the operation of devices with patterned gates depends crucially on the behavior of the exposed surface between the gates. It is generally assumed that the high density of surface states on GaAs causes the Fermi energy to be pinned, but it is not clear that this holds at low temperature. Also, the usual assumption that all donors are ionized is certainly inaccurate in GaAs/$Al_xGa_{1-x}As$ heterostructures, where donors can behave as deep levels (DX centers). Both the surface and the donors have strong effects on the potential seen by electrons in the 2DEG. An improved understanding of their behavior, and ways of testing models against experiments, are vital to improving the validity of simulations.

Unfortunately most measurements provide very indirect information on the potential seen by the electrons. A quantity that is relatively simple both to calculate and to measure is the threshold voltage, at which all active electrons are just driven out of the 2DEG.[6,7] Although theoretical and experimental values for threshold voltages sometimes agree, the differences are often large. This may mean that the surface has been treated incorrectly, but the high electric field generated by the gate may also be affecting the surface or the donors. A more direct measure of the potential seen by electrons in the 2DEG, for small voltages on the gates, would provide a clearer probe.

The commensurability oscillations[8–10] seen in the low-field magnetoresistance of a 2DEG under a lateral superlattice give a direct measurement of the periodic potential. The superlattice provides a one-dimensional periodic potential experienced by the electrons as they travel from source to drain along x. A schematic diagram is shown in Fig. 1. The periodic potential is provided by a pattern of parallel striped metal gates on the surface, perpendicular to the direction in which the electrons travel. Each gate has a length $2a$, the gaps between have width $2b$, and the depth of the electrons is d. A voltage Φ_g on the gates produces a periodic potential which is transmitted to the electrons in the 2DEG. A problem with any gated structure such as this is the separation d between the electrons and the gates on the surface, which smooths and weakens the periodic potential.

Commensurability oscillations depend on the ratio between the radius $R_c(B)$ of the cyclotron motion in a magnetic field and the period of the superlattice, $2(a+b)$. The origin of these oscillations is understood within both quantum-mechanical[11] and semiclassical[12] descriptions. The semiclassical theory[12] shows that the magnetoresistance $R(B)$ is given by

$$\frac{\delta R}{R} = \sum_{n=1}^{\infty} \left(\frac{v_n}{E_F}\right)^2 \left[\frac{nl^2}{2(a+b)R_c}\right] \cos^2\left[\frac{2\pi n R_c}{2(a+b)} - \frac{\pi}{4}\right], \tag{1.1}$$

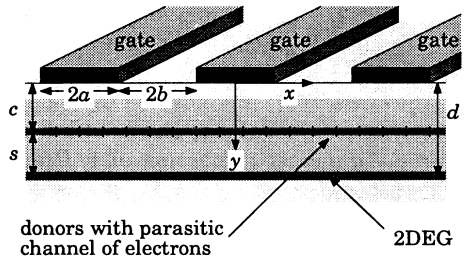

FIG. 1. Construction of superlattice used in the experiment. The donors lie in a plane c below the surface, surrounded by a parasitic layer of electrons. The 2DEG is a further distance s below the donors (which includes an allowance for the thickness of the 2DEG); $d = c + s$. The lengths of the gates and gaps are $2a$ and $2b$. The origin is chosen in the center of a gate, with x parallel to the surface in the direction of the current and y pointing downward.

where $R_c = mv_F/eB$ is the cyclotron radius, v_n is the amplitude of the nth harmonic of the periodic potential energy at the 2DEG, E_F and v_F are the Fermi energy and velocity, and l is the mean free path. Each harmonic contributes independently, and the phases of the harmonics of the potential are not reflected in the magnetoresistance. Most experimental data are adequately described by this model with a sinusoidal modulation potential.[13,14] This is because the 2DEG is formed deep below the surface (typically $d \approx 100$ nm) in conventional high-mobility layers, so higher-order Fourier components of the surface potential are strongly attenuated. More recent experiments[15] employed a superlattice device with a period of 270 nm on a shallow 2DEG at an interface only 28 nm below the surface. The improved coupling between the surface and the 2DEG made the shape of the periodic potential far from sinusoidal, and a strong second harmonic was seen.

In this paper we have tried to model the potential seen in these recent experiments. This is an advantageous structure, since the 2DEG is only weakly perturbed by the periodic potential, unlike devices such as quantum point contacts, where a large voltage on the gates depletes part of the 2DEG. It is usually assumed that the gates generate an electrostatic field that perturbs the electrons. A difficulty, discussed above, is that the boundary condition on the exposed GaAs between the metal gates is not well understood. It is usually assumed that surface states pin the Fermi energy on the surface. Our calculations show that this "pinned" boundary condition leads to a potential in the 2DEG containing almost no second harmonic, in disagreement with experiment. An alternative model is to assume that the surface charge cannot respond on the time scale of the experiment. This "frozen" boundary condition leads to a greater second harmonic, but which is still much smaller than in experiment. Thus electrostatics cannot predict the experimental result.

We have also calculated the effect of elastic strain. The gates are metallic (Au/Ti) and have a different coefficient of expansion from the GaAs underneath. Differential contraction sets up a strain field as the sample is cooled, which couples to the 2DEG through the deformation potential. This has been used intentionally to confine electrons for optical purposes with better-controlled stressors like $In_xGa_{1-x}AsP$[16] or $In_xGa_{1-x}As$.[17–19] This effect is unintentional in the superlattice, but we find that it gives the best explanation of the experimental data.

We briefly describe the experimental results in the next section, followed by the electrostatic calculations in Sec. III and strain in Sec. IV.

II. EXPERIMENTAL RESULTS

The schematic construction of the superlattice used in the recent experiment[15] is shown in Fig. 1. The x axis is parallel to the flow of current along the surface and y is downward, normal to the surface. The layers comprise a GaAs substrate, two 10 nm thick AlAs barriers separated by 2 nm of $Al_xGa_{1-x}As$ δ doped with Si to 4×10^{16} m^{-2}, and a 5.4 nm GaAs cap layer. The 2DEG is confined at an interface 28 nm deep. The extent of the wave function normal to this interface[20] is about 7–8 nm. This is much smaller than the period of the superlattice and will therefore be treated simply by adding it to the depth of the 2DEG, giving $d \approx 35$ nm. The gates were formed from 15 nm Ti/15 nm Au; their length was $2a = 130$ nm and the gaps were $2b = 140$ nm. The density of electrons in the gated region was 3.2×10^{15} m^{-2} with a mobility of about 40 m^2 V^{-1} s^{-1}, corresponding to a mean free path $l = 3.7\,\mu$m.

The mobility of electrons in these layers is surprisingly high for so thin a spacer. This is believed to be due to a parasitic channel of electrons around the δ-doped layer. Although these electrons have a low mobility and make a negligible direct contribution to transport, they screen

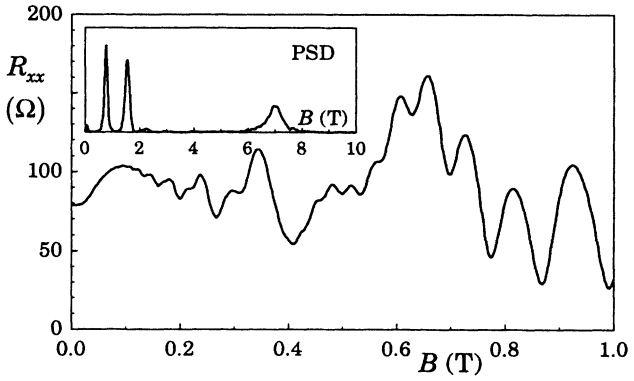

FIG. 2. Experimental result[15] for magnetoresistance as a function of magnetic field B. The commensurability oscillations occur for $B < 0.5$ T, and show a strong second harmonic content. This is confirmed by the power spectral density (PSD inset) obtained from a Fourier transform of the magnetoresistance considered as a function of $1/B$. The peaks at low frequency arise from commensurability oscillations, showing a strong fundamental and second harmonic but little third harmonic; the peak at 7–8 T is from the Shubnikov–de Haas effect.

the random potential due to the ionized donors and enhance the mobility of the 2DEG from an expected value of only about 6 $m^2 V^{-1} s^{-1}$ if the full random potential were operative. Although this means that the device performs far better than would otherwise be expected, it greatly complicates the analysis because it means that the potential from the gate is screened twice, by the electrons around the donors as well as by those in the 2DEG.

The magnetoresistance obtained for zero gate voltage is shown in Fig. 2. The commensurability oscillations occur for $B < 0.5$ T, with Shubnikov–de Haas oscillations at higher fields, and it is clear that a strong second harmonic is present. This is confirmed by the power spectral density shown in the inset, obtained by considering the magnetoresistance as a function of $1/B$ and making a Fourier transform. Equation (1.1) was used to deduce the periodic potential from the commensurability oscillations. The estimated strength of the Fourier components of the modulation $V^{\rm exp}(x)$ were found to be $v_1^{\rm exp} \approx 0.5$ meV for the fundamental (first harmonic) and $v_2^{\rm exp} \approx 0.3$ meV for the second harmonic. The third harmonic is barely seen. A sample reconstruction of $V^{\rm exp}(x)$ is plotted in Fig. 3(a). This assumes particular values for the phases, which cannot be recovered from the experiment; in particular it is impossible to tell whether the peaks in potential energy occur under the gates or gaps, and whether the double features are minima or maxima.

We shall now calculate this potential, first assuming that it is of electrostatic origin before considering elastic strain in Sec. IV.

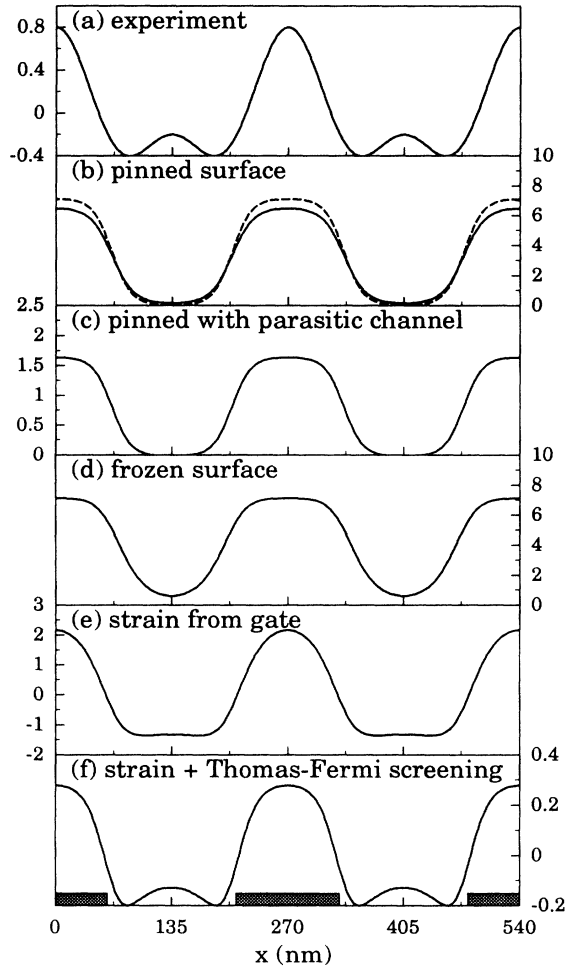

FIG. 3. Potential energy in the 2DEG under the superlattice, all in meV but with different scales. The gray rectangles show the position of the gates. (a) Deduced from experiment.[12,15] The phases of the Fourier components are unknown. The other curves are calculations using different models, assuming $\Phi_g = -0.1$ V for electrostatics and compression of $\varepsilon_{xx}^0 = -0.001$ on the surface for the strain. (b) Pinned surface with modified Thomas-Fermi screening (full line), and a purely electrostatic approximation (broken line). (c) Pinned surface, including the effect of the parasitic electrons around the sheet of donors. (d) Frozen surface, purely electrostatic calculation; note the asymmetry between the peaks and valleys. (e) Elastic strain before screening by the 2DEG. (f) Elastic strain reduced by Thomas-Fermi screening. This gives a strong double minimum whose shape is close to that of the experimental results, although the overall magnitude is slightly too small.

III. ELECTROSTATICS

The electrostatic field generated by patterned gates has been widely used to guide electrons since its first application to produce quantum wires.[1,2] An advantage of this form of superlattice is that the voltage on the gates Φ_g can readily be varied to tune the periodic potential seen by the 2DEG. In fact, the experiments on the superlattice were performed with $\Phi_g = 0$ but nonetheless reveal a periodic potential in the 2DEG. We must invoke a built-in voltage associated with the gates if the observed potential is of electrostatic origin. It turns out that no more than 0.1 V is needed, which is an acceptable number for the change in height of the Schottky barrier on the surface of GaAs when a metal is deposited,[21] and this acts as an effective gate voltage.

Another problem is the boundary condition to be applied to the free surface of GaAs between the gates. It is usually assumed that the Fermi energy E_F is pinned on free surfaces of GaAs.[22] This is unambiguous in equilibrium, where E_F is constant throughout the structure. However, it presents problems as soon as a bias is applied to the gates, even if no current flows, as it is no longer clear whether the surface is pinned to E_F in the 2DEG or to that in the gate. Clearly there would be no pattern in the 2DEG if the surface were pinned to the gate, as no difference between the gap and gate would be seen from inside the material.[7] It must therefore be assumed that the surface remains pinned to E_F in the 2DEG, which we take as the zero of energy and potential. This means that the exposed surface behaves as an equipotential at zero, a convenient boundary condition that gives simple electrostatics. This is the pinned model.

The difficulty with the pinned model is that charge must move from the 2DEG to the surface to keep its potential constant in response to a change in Φ_g. While this may pose no problem at room temperature, it seems unlikely at the low temperatures (around 1 K) at which

experiments on superlattices and quantum wires are usually performed. The charge on the surface may well be frozen under these conditions. Although the equipotential model can be used to calculate the density of electrons in the 2DEG at equilibrium at room temperature, the surface should instead be treated as a simple dielectric boundary, with a fixed charge density, in response to a change in Φ_g applied at low temperature. This is the frozen model. The high dielectric constant of semiconductors means that the boundary condition is approximately $\partial\phi/\partial n = 0$ in this case, the vanishing of the normal derivative, rather than $\phi = 0$.

A third problem arises from the parasitic channel of free electrons that is believed to exist around the plane of donors. These provide an additional source of screening beyond the effect of the 2DEG. We have treated this only for the case of a pinned surface.

The rest of this section contains four calculations of the potential in the 2DEG. First we consider the pinned model, and use Thomas-Fermi screening to treat the 2DEG. This is then extended to include further screening from the parasitic layer of electrons. The next calculation is again for a pinned surface but uses a purely electrostatic approximation. This exploits the good screening provided by the 2DEG to treat it as an equipotential surface, and has the advantage that it can be extended to more complicated geometries and boundary conditions. It is used in the final section to treat the frozen model, which is complicated by a mixed boundary condition on the surface. We write the electronic charge as $-e$.

A. Pinned surface with Thomas-Fermi screening

Start by calculating the potential $\Phi^g(x,y)$ from the gate alone. The potential on the surface is a square wave with $\Phi^g(x,0) = \Phi_g$ for $|x| < a$ and $\Phi^g(x,0) = 0$ otherwise within the fundamental period $|x| < (a+b)$. This can be expanded as a Fourier cosine series,

$$\Phi^g(x,0) = \tfrac{1}{2}\phi_0^g(0) + \sum_{m=1}^{\infty} \phi_m^g(0)\cos(q_m x), \tag{3.1}$$

with wave vectors $q_m = \pi m/(a+b)$ and coefficients $\phi_m^g(0) = [2\Phi_g/q_m(a+b)]\sin(q_m a)$. Upper-case letters are used for quantities in real space with corresponding lower-case letters for the Fourier series in x. Each Fourier coefficient decays exponentially with depth, so the coefficients at depth y are given by $\phi_m^g(y) = \phi_m^g(0)\exp(-q_m y)$. This emphasizes the importance of having a shallow structure with $d \ll (a+b)$ if higher harmonics are to be seen in the 2DEG.

This potential is screened by the 2DEG. The dielectric function of a 2DEG in the Thomas-Fermi approximation, which is adequate for the long wavelengths that concern us, is $\epsilon_{\rm TF}(q) = 1 + q_{\rm TF}/q = 1 + 2/(a_0 q)$ where the screening wave vector $q_{\rm TF} = 2/a_0$ and the effective Bohr radius is

$$a_0 = \frac{4\pi\epsilon\epsilon_0\hbar^2}{me^2}, \tag{3.2}$$

about 10 nm in GaAs. This form for $\epsilon_{\rm TF}(q)$ was derived[23] for a 2DEG surrounded by infinite regions; here we must correct for the pinned surface at $y = 0$. This reduces the effectiveness of screening at long wavelengths compared with the depth d of the electrons, giving

$$\epsilon_{\rm TF}(q,d) = 1 + \frac{2}{a_0 q}[1 - \exp(-2qd)]. \tag{3.3}$$

An important limit is $\epsilon_{\rm TF}(q=0,d) = 1 + 4d/a_0 \approx 16$ here; it does not diverge as for the 2DEG without boundaries. The Fourier coefficients of the screened potential energy $V^{\rm scr}(x)$ in the 2DEG are given by $v_m^{\rm scr} = -e\phi_m^g(d)/\epsilon_{\rm TF}(q_m,d)$. For $\Phi_g = -0.1$ V this gives $v_1^{\rm scr} = 3.6$ meV and $v_2^{\rm scr} = 0.14$ meV. The fundamental $v_1^{\rm scr}$ is much too large, and the second harmonic $v_2^{\rm scr}$ is too small. There would be no second harmonic at all if the gates and gaps were of equal length ($a = b$), and the experimental device differs only slightly from this condition. The potential energy $V^{\rm scr}(x)$ is plotted in Fig. 3, and the near symmetry between the peaks and valleys reflects the weak second harmonic.

Although this estimate is based on a very rough estimate for Φ_g, it can be improved if we account for the electrons that surround the plane of donors.

B. Effect of parasitic channel

As mentioned in Sec. II, it is believed that there are free electrons around the plane of donors in the experimental structure. These will also screen the potential from the gates on the surface and reduce it below the estimate of the previous section. We shall assume that the electrons in this parasitic channel form another two-dimensional electron gas, trapped in the potential well produced by the ionized donors. Although its mobility is far below that of the "intended" 2DEG, so it does not contribute significantly to transport, it can screen the static potential from the gates. More than one electric subband may be occupied, in which case the screening will be more effective than calculated here.

The situation is shown in Fig. 1. The parasitic layer lies a distance c below the surface, separated from the 2DEG by s, with $d = c + s$. Consider a single Fourier component q_m of charge and potential in the plane. The total change in potential energy in the 2DEG is $v_m^{\rm par}$, which includes $-e\phi_m^g(d)$ from the gate (the external potential) and contributions from polarization in the two planes of electrons. This induces a Fourier component of areal charge density σ_m. A superscript "(p)" is added to denote the parasitic layer. According to the Thomas-Fermi approximation, the charge density induced in the 2DEG, σ_m, is given in terms of the total potential energy $v_m^{\rm par}$ by

$$\sigma_m = e\frac{m}{\pi\hbar^2}v_m^{\rm par}. \tag{3.4}$$

This charge density in the plane $y = d$ produces a potential whose Fourier components are

$$\phi_m(y) = \frac{\sigma_m}{2\epsilon\epsilon_0 q_m}(e^{-q_m|y-d|} - e^{-q_m|y+d|}); \tag{3.5}$$

the first exponential is the direct potential and the second is an image added to satisfy the equipotential boundary condition on the surface. The total self-consistent potential energy in the 2DEG is given by

$$v_m^{\rm par} = -e\phi_m^g(d) - \frac{e\sigma_m^{(p)}}{2\epsilon\epsilon_0 q_m}(e^{-q_m s} - e^{-q_m(s+2c)}) - \frac{e\sigma_m}{2\epsilon\epsilon_0 q_m}\left(1 - e^{-2q_m d}\right), \quad (3.6)$$

where the first term is the external potential, the second arises from polarization of the parasitic layer and the third is from polarization of the 2DEG. Using Eq. (3.4) and the analog for $\sigma_m^{(p)}$ gives

$$\begin{aligned} v_m^{\rm par} &= -e\phi_m^g(d) - \frac{2}{a_0 q_m}e^{-q_m s}\left(1 - e^{-2q_m c}\right)v_m^{(p)} - \frac{2}{a_0 q_m}\left(1 - e^{-2q_m d}\right)v_m^{\rm par}, \\ &= -e\phi_m^g(d) - [\epsilon_{\rm TF}(q_m, c) - 1]e^{-q_m s}v_m^{(p)} - [\epsilon_{\rm TF}(q_m, d) - 1]v_m^{\rm par}, \end{aligned} \quad (3.7)$$

which has been simplified by introducing the Bohr radius [Eq. (3.2)] and the definition of the modified Thomas-Fermi dielectric function [Eq. (3.3)]. Similarly, the total potential energy in the parasitic layer is

$$v_m^{(p)} = -e\phi_m^g(c) - [\epsilon_{\rm TF}(q_m, c) - 1]v_m^{(p)} - [\epsilon_{\rm TF}(q_m, c) - 1]e^{-q_m s}v_m^{\rm par}. \quad (3.8)$$

Eliminating $v_m^{(p)}$ between these gives $v_m^{\rm par} = -e\phi_m^g(d)/\epsilon_{\rm eff}(q_m)$ where the effective dielectric function is

$$\epsilon_{\rm eff}(q) = \epsilon_{\rm TF}(q, c)\epsilon_{\rm TF}(q, d) - e^{-2qs}[\epsilon_{\rm TF}(q, c) - 1]^2. \quad (3.9)$$

This effective dielectric function has two simple limits. The first is where the parasitic channel is just under the surface ($c = 0$, $d = s$). The parasitic channel can do nothing in this limit because the potential on the surface is imposed as a boundary condition. Now $\epsilon_{\rm TF}(q, c = 0) = 1$ so Eq. (3.9) reduces to $\epsilon_{\rm eff}(q) = \epsilon_{\rm TF}(q, d)$ which is the correct result as if no parasitic layer were present. The second limit is when the 2DEG and the parasitic channel of electrons coincide ($s = 0$, $d = c$), so there are still two sheets of electrons that screen the potential but they lie in the same plane. Thus we should get a result similar to that for a single 2DEG [Eq. (3.3)], but the polarizability $(\epsilon - 1)$ should be doubled to allow for the two planes of electrons. Indeed, Eq. (3.9) reduces in this limit to $\epsilon_{\rm eff}(q) = 2[\epsilon_{\rm TF}(q, d) - 1] + 1$.

Returning to the layers in Fig. 1 with $\Phi_g = -0.1$ V, we get $v_1^{\rm par} = 0.95$ meV and $v_2^{\rm par} = 0.04$ meV. The magnitude of $v_1^{\rm par}$ is now close to experiment but $v_2^{\rm par}$ is far too small. This is confirmed by the plot of $V^{\rm par}(x)$ in Fig. 3, and indicates that electrostatics with a pinned surface is unable to explain the shape of the potential deduced from the experiment.

C. Pinned surface with pure electrostatics

Although the results of the previous two sections show that the pinned surface cannot explain this particular experiment, we give here another way of calculating the potential induced in the 2DEG because it of general usefulness and relates closely to the method that we use in the following section to treat the frozen surface. It is a purely electrostatic calculation in which the dielectric function of the 2DEG is not introduced explicitly.

Consider first a uniform gate rather than a superlattice and make a small uniform change in the density of electrons in the 2DEG, $\delta n_{\rm 2D}$. This changes the Fermi energy, expressed as a voltage, by $\delta\Phi_F = \delta E_F/e = (1/e)(\pi\hbar^2/m)\delta n_{\rm 2D}$. It also changes the electrostatic potential between the gate and 2DEG by $e\delta n_{\rm 2D}d/(\epsilon\epsilon_0)$. The measured voltage between the gate and 2DEG changes by the sum of these, $\delta\Phi_g$. The ratio of this to the change in Fermi voltage is

$$\frac{\delta\Phi_g}{\delta\Phi_F} = 1 + \frac{me^2 d}{\pi\epsilon\epsilon_0\hbar^2} = 1 + \frac{4d}{a_0}. \quad (3.10)$$

This is just the limit as $q \to 0$ of the modified Thomas-Fermi dielectric function, Eq. (3.3), and is around 16 for the experimental structure. This large number means that the dominant energies in the system are electrostatic rather than kinetic. It should therefore be a good approximation to neglect the kinetic energy and assume that the 2DEG screens the potential perfectly, $\delta\Phi_F = 0$. This means that we solve the electrostatic problem in the region between the surface and the 2DEG, treating the 2DEG as an equipotential at zero. We can then calculate the normal field on the 2DEG, use Gauss's theorem to deduce the charge density, and thus calculate the change in Fermi energy of the 2DEG. If the normal electric field is $E_y(x)$, the same arguments as those for Eq. (3.10) lead to a change in potential energy in the 2DEG of

$$V(x) = -\tfrac{1}{4}ea_0E_y(x). \quad (3.11)$$

We can now apply this to the superlattice and calculate the potential $\Phi(x, y)$ in the region between the surface and the 2DEG. The potential on the surface, $\Phi^g(x, 0)$, was written as a Fourier series in Eq. (3.1). This needs to be extended as a function of y, respecting the boundary condition $\Phi = 0$ on the 2DEG at $y = d$. The Fourier coefficients of the potential as a function of depth are given by

$$\phi_m(y) = \frac{\sinh[q_m(d - y)]}{\sinh(q_m d)}\phi_m^g(0), \quad (3.12)$$

taking the limit for $m = 0$. The derivative with respect to y at $y = d$ gives E_y, and substituting into Eq. (3.11) gives the self-consistent (screened) potential energy $v_m^{\rm eq}$ in the 2DEG,

$$v_m^{\rm eq} = -e\phi_m^g(0)\frac{q_m a_0}{4\sinh(q_m d)}. \quad (3.13)$$

The numerical values for $\Phi_g = -0.1$ V are $v_1^{\rm eq} = 4.1$ meV

and $v_2^{\rm eq} = 0.18$ meV. These are close to those obtained using Thomas-Fermi screening in Sec. III A, but a little higher because we have neglected the "+1" on the right-hand side of Eq. (3.10).

D. Frozen surface

In this case we have only been able to obtain a solution analogous to the electrostatic one of the previous section. The reason is that the boundary condition on the surface is now mixed, which complicates the electrostatics. Consider the unit cell about the origin, $|x| \le (a+b)$ and $0 \le y \le d$. The electrostatic potential $\Phi(x,y)$ must satisfy

$$\Phi(x,0) = \Phi_g, \qquad |x| < a, \tag{3.14a}$$

$$\left.\frac{\partial\Phi}{\partial y}\right|_{y=0} = 0, \qquad |x| > a, \tag{3.14b}$$

$$\Phi(x,d) = 0, \tag{3.14c}$$

$$\left.\frac{\partial\Phi}{\partial x}\right|_{x=\pm(a+b)} = 0. \tag{3.14d}$$

The fourth of these follows from the periodicity of the superlattice (and also holds at $x = 0$).

The solution uses conformal mapping and the elliptic integral of the first kind (Ref. 24, Sec. 7.6, whose notation we follow). The technique is standard and will only be outlined here. A first mapping $p = \mathrm{sn}(z/C, k_1)$ uses the elliptic function to expand the rectangular unit cell in $z = x + iy$ into the upper half plane of p. This requires a parameter k_1 and a scale factor C that obey

$$CK(k_1) = (a+b); \qquad CK'(k_1) = d. \tag{3.15}$$

An elliptic integral is then used to map the half plane back into a rectangle in the w plane, with $p = (k_2/k_1)\mathrm{sn}(w,k_2)$. The parameter of this mapping is

$$k_2 = k_1 \mathrm{sn}\left(\frac{a}{C}, k_1\right), \tag{3.16}$$

and the rectangle has $|\mathrm{Re}w| \le K(k_2)$ and $0 \le \mathrm{Im}w \le K'(k_2)$. After these two mappings the equipotential regions [Eqs. (3.14a) and (3.14c)] occupy the two horizontal edges of the rectangle, while the boundaries with vanishing normal derivative [Eqs. (3.14b) and (3.14d)] are brought together to fill each of the two vertical edges. The electrostatic problem is trivial in this plane, giving $\Phi = \Phi_g[1 - \mathrm{Im}w/K'(k_2)]$. The normal electric field, $\partial\Phi/\partial y$, on the line $y = d$ is then used to find the screened potential energy in the 2DEG from Eq. (3.11). The final result is

$$V^{\rm fr}(x) = -e\Phi_g \frac{a_0}{4d}\frac{K'(k_1)}{K'(k_2)}\sqrt{\frac{1-k_1^2\mathrm{sn}^2(x/C,k_1)}{1-k_2^2\mathrm{sn}^2(x/C,k_1)}}. \tag{3.17}$$

This is plotted in Fig. 3 for $\Phi_g = -0.1$ V. There is now a clear asymmetry which holds even if $a = b$, with broad peaks under the gates and narrow valleys under the gaps. This is confirmed by the Fourier coefficients which were extracted numerically, giving $v_1^{\rm fr} = 3.6$ meV and $v_2^{\rm fr} = -0.4$ meV. The numbers will be reduced if we allow for screening by electrons in the parasitic layer. Although the relative content of second harmonic in the potential, $|v_2^{\rm fr}/v_1^{\rm fr}|$, is now much greater than for the pinned surface, it is still well below the experimental value.

We have to conclude that electrostatics is unable to explain the experimental results, even with the different boundary conditions, and now turn to elastic strain as a different means of patterning the 2DEG.

IV. STRAIN

The electrostatic potential is applied to the 2DEG through metal gates on the surface of the GaAs. These are composed of a layer of Ti with a further layer of Au on top.[15] The gates are usually deposited by evaporation which takes place at a high temperature, although it is difficult to know the precise conditions that prevail during deposition. The coefficients of expansion α of GaAs and Ti are close to each other at room temperature[25,26] ($\alpha_{\rm GaAs} \approx 6.8\times10^{-6}$ and $\alpha_{\rm Ti} \approx 8.3\times10^{-6}$), but their low-temperature behavior is different; the average values are $\alpha_{\rm GaAs} \approx 4\times10^{-6}$ and $\alpha_{\rm Ti} \approx 7\times10^{-6}$ as the temperature decreases from 300 K to 4.2 K. As a result, Ti shrinks by a fraction of about 10^{-3} with respect to GaAs at helium temperature. The deformation potential constant $\Xi \approx -8$ eV, so the amplitude of the bare potential acting on electrons in the 2DEG may approach 8 meV in a shallow structure. Screening will reduce this to about 1 meV, which is of the magnitude observed in experiment, so strain is a plausible mechanism. We shall calculate the strain field analytically in this section and deduce the potential energy in the 2DEG, first for a single gate where numerical calculations are available for comparison, and then for the array of gates. First we give the general elastic theory needed.

A. General elastic theory

We shall assume that the system is translationally invariant in the dimension normal to the cross section of Fig. 1, so that all stresses σ and strains ε depend only on x and y. Under this assumption there is no normal strain along the length of gates, $\varepsilon_{zz} = 0$, but the stress σ_{zz} does not vanish. The normal stresses and strains are related by $E\varepsilon_{xx} = \sigma_{xx} - \nu(\sigma_{yy} + \sigma_{zz})$ and permutations, where E is Young's modulus and ν is Poisson's ratio. Setting $\varepsilon_{zz} = 0$ and eliminating σ_{zz} gives

$$E\varepsilon_{xx} = (1-\nu^2)\sigma_{xx} - \nu(1+\nu)\sigma_{yy} \tag{4.1}$$

and similarly for ε_{yy}. The stress can be deduced[27] from a function $\chi(x,y)$ that obeys the biharmonic equation, $\nabla^2\nabla^2\chi = 0$; the components are given by

$$\sigma_{xx} = \frac{\partial^2\chi}{\partial y^2}, \quad \sigma_{xy} = -\frac{\partial^2\chi}{\partial y\partial x}, \quad \sigma_{yy} = \frac{\partial^2\chi}{\partial x^2}. \tag{4.2}$$

The dilation δ, which affects the electrons through the deformation potential, is given by

$$E\delta = E(\varepsilon_{xx} + \varepsilon_{yy}) = (1+\nu)(1-2\nu)(\sigma_{xx} + \sigma_{yy}), \quad (4.3)$$

and Eq. (4.2) shows that $\sigma_{xx} + \sigma_{yy} = \nabla^2\chi$.

We take the boundary conditions on σ and χ to be as follows:

$$\sigma_{xx} = \frac{\partial^2\chi}{\partial y^2} = \frac{E}{1-\nu^2}\varepsilon^0_{xx} \quad \text{under the gates,} \quad (4.4a)$$

$$\sigma_{xy} = -\frac{\partial^2\chi}{\partial y \partial x} = 0 \quad \text{between the gates,} \quad (4.4b)$$

$$\sigma_{yy} = \frac{\partial^2\chi}{\partial x^2} = 0 \quad \text{everywhere at } y = 0, \quad (4.4c)$$

$$\chi = 0 \quad \text{at } y = \infty. \quad (4.4d)$$

The main assumption is that there is no relaxation of the gate. This requires that the gate is thin enough that we can neglect any stress σ_{yy} due to bending of the gates, but thick enough that we can neglect variations in ε_{xx} caused by stress in the GaAs acting back on the gate; we shall check this briefly in Sec. IV D. Then Eq. (4.4a) follows from Eq. (4.1) as well as the assumption that the strain parallel to the surface is uniform under the gate with a value ε^0_{xx}. Condition (4.4b) states that there can be no shear stress at a free surface, while Eq. (4.4c) requires a thin gate. The problem can be simplifed by writing $\chi = y\phi$, where ϕ satisfies Laplace's equation and the following boundary conditions:

$$2\frac{\partial\phi}{\partial y} = \frac{E}{1-\nu^2}\varepsilon^0_{xx} \quad \text{under the gates,} \quad (4.5a)$$

$$\frac{\partial\phi}{\partial x} = 0 \quad \text{between the gates,} \quad (4.5b)$$

$$\phi = 0 \quad \text{at } y = \infty. \quad (4.5c)$$

Boundary condition (4.4c) is satisfied trivially. The dilation is given by

$$\delta = \frac{2(1+\nu)(1-2\nu)}{E}\frac{\partial\phi}{\partial y}. \quad (4.6)$$

The problem of calculating ϕ is now closely related to the electrostatic problems that we have solved in Sec. III; condition (4.5a) is like a constant charge density under the gate, while (4.5b) shows that the rest of the surface behaves as an equipotential, the reverse of their roles in the true electrostatic problem. The value of the equipotential is unknown and should be adjusted so that the solution obeys Eq. (4.5c), but we shall ignore this, since we need only the derivative of ϕ. Again, conformal transformation can be used to solve the problem, and we shall first do this for a single gate to allow comparison with previous numerical results.

B. Single gate

Consider a single gate between $x = \pm a$ on the surface of GaAs. We have to find a solution to Laplace's equation with the following boundary conditions on the surface, $y = 0$:

$$\frac{\partial\phi}{\partial y} = \frac{E}{2(1-\nu^2)}\varepsilon^0_{xx} = A \text{ (say)}, \quad |x| < a, \quad (4.7a)$$

$$\frac{\partial\phi}{\partial x} = 0, \quad |x| > a, \quad (4.7b)$$

and ϕ must vanish at infinity. The solution is written as the imaginary part of a complex function $w = u + iv$,

$$\phi = A\,\mathrm{Im}w; \qquad w = z - \sqrt{z^2 - a^2}. \quad (4.8)$$

The branch cut of the square root is chosen so that $\mathrm{Im}\sqrt{z^2-a^2} > 0$ on the positive y axis. The first term, z, satisfies the boundary conditions on $y = 0$; in particular, it generates the field under the gate. However it gives the wrong behavior at infinity and this is corrected by the second term, which obeys Eq. (4.7b) and gives $\partial\phi/\partial y = 0$ under the gate. Thus the sum satisfies all the boundary conditions.

The dilation needs $\partial\phi/\partial y = A\partial v/\partial y = A\mathrm{Re}dw/dz$. Thus, using Eqs. (4.6) and (4.7a), the potential energy seen in the 2DEG at a depth y is

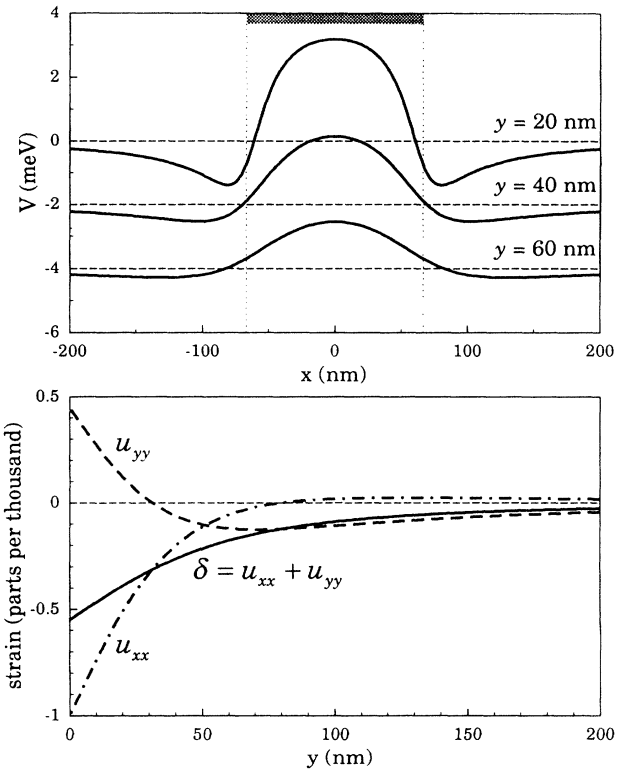

FIG. 4. Strain under a single gate of width $2a = 130$ nm. (a) Potential energy caused by dilation as a function of x at depths of $y = 20$, 40, and 60 nm, with vertical scales offset as shown by the broken lines. The central region is in compression, giving a positive potential energy, but this changes sign near the edges of the gate, marked by a gray rectangle. (b) Dilation (full line) and individual components of strain as a function of depth y under the middle of the gate, $x = 0$. The dilation decays monotonically but the individual components of strain change sign as a function of depth. The strain under the gate is $\varepsilon^0_{xx} = -0.001$ (GaAs in compression).

$$V^{\rm str}(x) = \Xi\delta(x,y) = \Xi\varepsilon^0_{xx}\frac{1-2\nu}{1-\nu}{\rm Re}\frac{dw}{dz}, \tag{4.9}$$

$$= \Xi\varepsilon^0_{xx}\frac{1-2\nu}{1-\nu}{\rm Re}\left(1-\frac{z}{\sqrt{z^2-a^2}}\right). \tag{4.10}$$

This is plotted in Fig. 4 for $\varepsilon^0_{xx} = -0.001$ and[25] $\nu = 0.31$. Qualitative comparison with numerical results[16,17,19] is excellent, although there are some quantitative differences because we have not allowed for relaxation of the stressor. Our curves are inverted with respect to these calculations because their stressors put the GaAs substrate into tension rather than compression as in our case. There is a region of compression (negative dilation) under the gate, which changes sign near the edge of the gate before decaying. The dilation under the middle of the gate decays monotonically as a function of depth but the individual components of strain both change sign.

C. Array of gates

The stress field under the periodic array of gates can be found in a similar way to the electrostatic solution with a frozen surface. As in Eq. (4.7), the boundary conditions on ϕ are that $\partial\phi/\partial y = A$ under the gates and $\partial\phi/\partial x = 0$ or $\phi =$ constant in the gaps between. By symmetry, we also know that the normal derivative $\partial\phi/\partial x = 0$ under the midpoints of the gates and the gaps. As for the single gate, we seek a complex potential $\phi = A\,{\rm Im}w$. Again a linear term $w = z$ satisfies the boundary conditions on $y = 0$ but not that at infinity and a correction must be found. The method (Ref. 28, pp. 90–91) is almost identical to Sec. III D, but is rather simpler because the region extends to infinity rather than being a finite rectangle terminated by the 2DEG, and trigonometric functions are adequate.

A first mapping, $p = \cos[\frac{1}{2}\pi z/(a+b)]$, expands the unit cell (a semi-infinite strip in z) into the upper half plane of p. The second, $p = \cos[\frac{1}{2}\pi a/(a+b)]\cos(w/B)$, restores the unit cell to a strip in w. The boundaries with vanishing normal derivative (the gates and the lines of symmetry) now lie next to each other on the infinite vertical edges, and the short horizontal edge is purely an equipotential corresponding to the gap between the gates, so the potential is trivially given by Imw as required. The constant B is adjusted to cancel the divergence of $w = z$ at infinity, and the total complex potential becomes

$$w = z - \frac{2(a+b)}{\pi}\arccos\frac{\cos[\frac{1}{2}\pi z/(a+b)]}{\cos[\frac{1}{2}\pi a/(a+b)]}. \tag{4.11}$$

This result reduces simply to that for a single gate [Eq. (4.8)] in the limit $b\to\infty$. For the dilation we need

$$\frac{dw}{dz} = 1 - \frac{\sin[\frac{1}{2}\pi z/(a+b)]}{\sqrt{\sin^2[\frac{1}{2}\pi z/(a+b)] - \sin^2[\frac{1}{2}\pi a/(a+b)]}}. \tag{4.12}$$

The potential energy in the 2DEG is then given by Eq. (4.9). This is plotted in Fig. 3. The features clearly follow from those of the single gate: a barrier under each gate, changing sign near the edges to give a double minimum under each gap. Thomas-Fermi screening by the electrons in the 2DEG, according to Eq. (3.3), reduces the potential and gives Fourier coefficients of $v_1^{\rm str} = 0.24$ meV and $v_2^{\rm str} = 0.10$ mV. The potential energy is plotted as a function of x in Fig. 3 and clearly agrees well with experiment. The ratio $|v_2^{\rm str}/v_1^{\rm str}| \approx 0.4$ which is close to the experimental value of 0.6; the magnitudes themselves are rather too small but we view the agreement as good given the lack of information needed to determine ε^0_{xx}. Screening due to the parasitic layer of electrons can also be included, as in Sec. III B. It has little effect on the shape but reduces the magnitude of the potential by a further factor of 4.

A remaining puzzle is the third harmonic of the potential. The third harmonic has about 0.4 the weight of the second harmonic in our calculation (Table I), but it is almost absent from the experimental measurement. This apart, we have shown that strain due to differential contraction between the Ti gates and the GaAs provides an acceptable explanation of the potential measured by the commensurability oscillations, superior to any of our results based on electrostatics.

D. Strain under the gate

Finally, we need to check the assumption that the Ti gates are uniformly strained. At equilibrium, the stresses at the interface between the Ti gate and GaAs obey the general relation[27]

TABLE I. First, second, and third harmonics of the potential in the 2DEG observed in experiment[15] and calculated using different models.

Model	v_1 (meV)	v_2 (meV)	v_3 (meV)	$\lvert v_2/v_1\rvert$
Experiment	±0.5	±0.3	<0.1	0.6
Pinned surface, no screening	28.1	0.73	−1.8	0.03
Pinned surface, Thomas-Fermi	3.6	0.14	−0.47	0.04
Pinned with parasitic channel	0.95	0.04	−0.15	0.04
Frozen surface	3.6	−0.44	−0.37	0.11
Strain	1.9	0.49	−0.16	0.26
Strain, screened	0.24	0.10	−0.04	0.40
Strain with parasitic channel	0.064	0.028	−0.013	0.44

$$h\frac{\partial\sigma_{xx}^{\mathrm{Ti}}}{\partial x}=\sigma_{xy}^{\mathrm{GaAs}}, \tag{4.13}$$

which applies to a thin film of thickness $h \ll a$. Using Eq. (4.1) to eliminate $\sigma_{xx}^{\mathrm{Ti}}$, and assuming that the film is so thin that $\sigma_{yy}=0$, gives

$$\frac{\partial\varepsilon_{xx}^{\mathrm{Ti}}}{\partial x}=\frac{(1-\nu_{\mathrm{Ti}}^2)G_{\mathrm{GaAs}}}{hE_{\mathrm{Ti}}}\varepsilon_{xy}^{\mathrm{GaAs}}, \tag{4.14}$$

where G_{GaAs} is the shear modulus of GaAs. We assumed earlier that the gate was uniformly strained, so the right-hand side of this equation must be small. For an estimate, put $\partial\varepsilon_{xx}/\partial x \approx \varepsilon^0/a$ and $\varepsilon_{xy} \approx \varepsilon^0$ where ε^0 is a rough measure of the strain. Then a dimensionless measure of the variation in strain is given by

$$a\frac{\partial\varepsilon_{xx}}{\partial x}\approx\lambda=\frac{a(1-\nu_{\mathrm{Ti}}^2)G_{\mathrm{GaAs}}}{hE_{\mathrm{Ti}}}. \tag{4.15}$$

For $h = 30\,\mathrm{nm}$ and $a = 70\,\mathrm{nm}$ we get $\lambda \approx 1.6$, which is not as small as we would like. Fortunately, numerical calculations[29] show that the qualitative behavior of the strain distribution remains the same at $\lambda < 5$. The limiting case of extremely large λ can be solved with a Wiener-Hopf approach but we defer this calculation to a further publication,[29] where we also consider the anisotropy of GaAs. The analytic calculation therefore appears adequate, given that the uncertainty in ε_{xx}^0 means that we cannot expect precise agreement with experiment.

V. CONCLUSIONS

We have calculated the potential generated in a 2DEG by a lateral surface superlattice, considering both electrostatics and elastic strain, and the results of the different models are summarized in Table I. The original aim of this work had been to discriminate between a pinned and frozen surface in the electrostatic calculation, but it proved that neither of these models could explain the experimental data.[15] The strain field produced by differential contraction between the metal gates and semiconductor, however, fits the data within a factor of 2 which we feel to be excellent agreement given that the deposition conditions are not known precisely. Strain also explains immediately why a periodic potential is present even when the gates are tied to ground and no electrostatic field is expected; this has been seen in other experiments that used a gate to apply the periodic potential.[10,13] The total potential with a bias applied to the gate should be given by a superposition of our results; such an analysis is under way.

Although strain has been used to pattern semiconductors on a submicrometer scale for optical purposes,[16–19] it is more difficult to detect strain through electronic transport because of the small potentials that result after screening. The commensurability oscillations are unusual in that small periodic potentials give rise to large effects in the magnetoresistance, making the effects of strain visible. Very much larger potentials would be needed to deplete and pattern a 2DEG into a wire, requiring enormous strains if coupling is through the deformation potential. Another possible route would be to harness the piezoelectric coupling, which in principle is capable of generating much larger potentials, but the high symmetry of GaAs must be defeated for this.

ACKNOWLEDGMENTS

This work was partly supported by U. K. SERC Grant No. GR/H44714. We are grateful to R. Cuscó, S. P. Beaumont, and A. R. Long for many useful discussions. It is also a pleasure to thank R. Cuscó for a close reading of the manuscript.

[1] T. J. Thornton, M. Pepper, H. Ahmed, D. Andrews, and G. J. Davies, Phys. Rev. Lett. **56**, 1198 (1986).
[2] H. Z. Zheng, H. P. Wei, D. C. Tsui, and G. Weimann, Phys. Rev. B **34**, 5635 (1986).
[3] D. A. Wharam, *et al.*, J. Phys. C **21**, L209 (1988).
[4] B. J. van Wees, H. van Houten, C. W. J. Beenakker, J. G. Williamson, L. P. Kouwenhoven, D. van der Marel, and C. T. Foxon, Phys. Rev. Lett. **60**, 848 (1988).
[5] J. A. Nixon, J. H. Davies, and H. U. Baranger, Phys. Rev. B **43**, 12 638 (1991).
[6] J. H. Davies, Semicond. Sci. Technol. **3**, 995 (1988).
[7] S. E. Laux, D. J. Frank, and F. Stern, Surf. Sci. **196**, 101 (1988).
[8] D. Weiss, K. von Klitzing, K. Ploog, and G. Weimann, Europhys. Lett. **8**, 179 (1989).
[9] R. R. Gerhardts, D. Weiss, and K. von Klitzing, Phys. Rev. Lett. **62**, 1173 (1989).
[10] R. W. Winkler, J. P. Kotthaus, and K. Ploog, Phys. Rev. Lett. **62**, 1177 (1989).
[11] C. Zhang and R. R. Gerhardts, Phys. Rev. B **41**, 12 850 (1990).
[12] C. W. J. Beenakker, Phys. Rev. Lett. **62**, 2020 (1989).
[13] P. H. Beton, E. S. Alves, P. C. Main, L. Eaves, M. W. Dellow, M. Henini, O. H. Hughes, S. P. Beaumont, and C. D. W. Wilkinson, Phys. Rev. B **42**, 9229 (1990).
[14] P. H. Beton, M. W. Dellow, P. C. Main, E. S. Alves, L. Eaves, S. P. Beaumont, and C. D. W. Wilkinson, Phys. Rev. B **43**, 9980 (1991).
[15] R. Cuscó, M. C. Holland, J. H. Davies, I. A. Larkin, E. Skuras, A. R. Long, and S. P. Beaumont, Surf. Sci. (to be published).
[16] K. Kash, R. Bhat, D. D. Mahoney, P. S. D. Lin, A. Schere, J. M. Worlock, B. P. Van der Gag, M. Koza, and P. Grabbe, Appl. Phys. Lett. **55**, 681 (1989).
[17] I.-H. Tan, D. Lishan, R. Mirin, V. Jayaraman, T. Yasuda, E. Hu, and J. Bowers, Appl. Phys. Lett. **59**, 1875 (1991).
[18] I.-H. Tan, T. Yasuda, R. Mirin, D. Lishan, E. L. Hu, J. Bowers, and J. Merz, J. Vac. Sci. Technol. A **10**, 664 (1992).

[19] I.-H. Tan, M. Y. He, J. C. Yi, E. Hu, N. Dagli, and A. Evans, J. Appl. Phys. **72**, 546 (1992).
[20] F. Stern and S. Das Sarma, Phys. Rev. B **30**, 840 (1984).
[21] S. M. Sze, *Physics of Semiconductor Devices* (Wiley, New York, 1981).
[22] R. B. Darling, Phys. Rev. B **43**, 4071 (1991).
[23] F. Stern, Phys. Rev. Lett. **18**, 546 (1967).
[24] J. Mathews and R. L. Walker, *Mathematical Methods of Physics* (Benjamin, Menlo Park, CA, 1970).
[25] R. I. Cottam and G. A. Saunders, J. Phys. C **6**, 2105 (1973).
[26] M. Kutz, *Mechanical Engineer's Handbook* (Wiley, New York, 1986).
[27] L. D. Landau, E. M. Lifshitz, A. M. Kosevich, and L. P. Pitaevskii, *Theory of Elasticity* (Pergamon, Oxford, 1986).
[28] W. R. Smythe, *Static and Dynamic Electricity*, (McGraw-Hill, New York, 1950).
[29] V. V. Tvardovskii and I. A. Larkin, *Strain Distribution in an Anisotropic Half-Space Under an Elastic Plate on its Surface* (private communication).

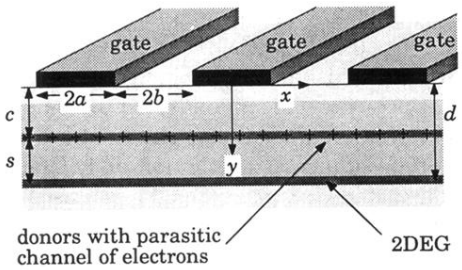

FIG. 1. Construction of superlattice used in the experiment. The donors lie in a plane c below the surface, surrounded by a parasitic layer of electrons. The 2DEG is a further distance s below the donors (which includes an allowance for the thickness of the 2DEG); $d = c + s$. The lengths of the gates and gaps are $2a$ and $2b$. The origin is chosen in the center of a gate, with x parallel to the surface in the direction of the current and y pointing downward.

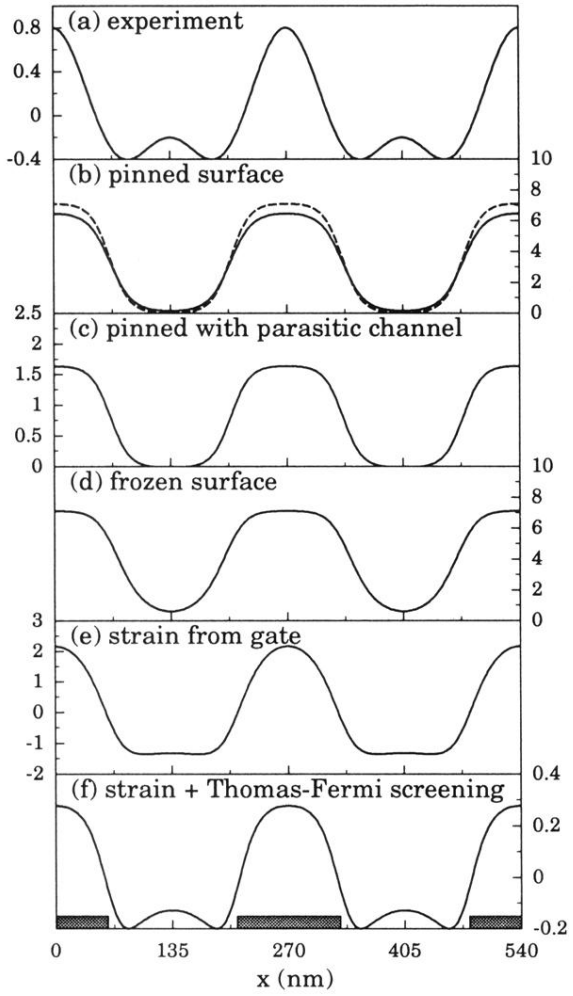

FIG. 3. Potential energy in the 2DEG under the superlattice, all in meV but with different scales. The gray rectangles show the position of the gates. (a) Deduced from experiment.[12,15] The phases of the Fourier components are unknown. The other curves are calculations using different models, assuming $\Phi_g = -0.1$ V for electrostatics and compression of $\varepsilon^0_{xx} = -0.001$ on the surface for the strain. (b) Pinned surface with modified Thomas-Fermi screening (full line), and a purely electrostatic approximation (broken line). (c) Pinned surface, including the effect of the parasitic electrons around the sheet of donors. (d) Frozen surface, purely electrostatic calculation; note the asymmetry between the peaks and valleys. (e) Elastic strain before screening by the 2DEG. (f) Elastic strain reduced by Thomas-Fermi screening. This gives a strong double minimum whose shape is close to that of the experimental results, although the overall magnitude is slightly too small.

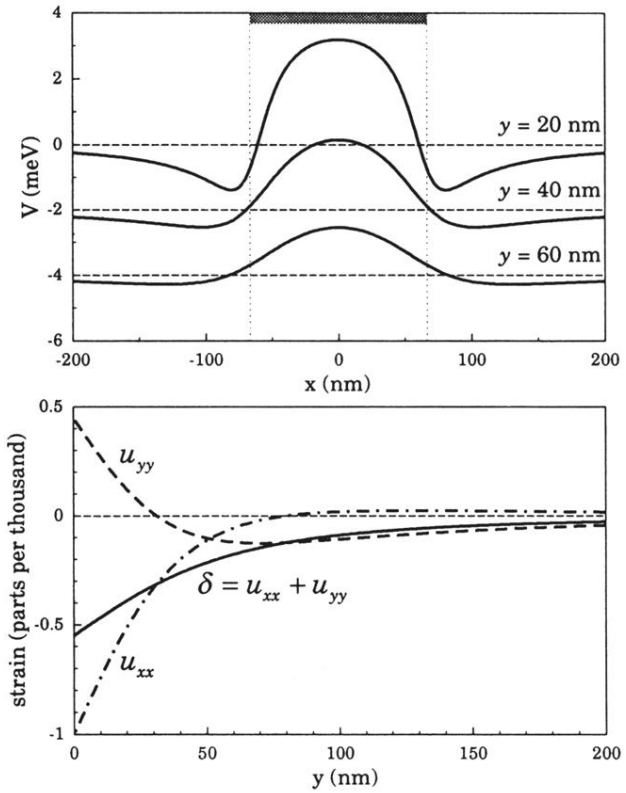

FIG. 4. Strain under a single gate of width $2a = 130$ nm. (a) Potential energy caused by dilation as a function of x at depths of $y = 20$, 40, and 60 nm, with vertical scales offset as shown by the broken lines. The central region is in compression, giving a positive potential energy, but this changes sign near the edges of the gate, marked by a gray rectangle. (b) Dilation (full line) and individual components of strain as a function of depth y under the middle of the gate, $x = 0$. The dilation decays monotonically but the individual components of strain change sign as a function of depth. The strain under the gate is $\varepsilon^0_{xx} = -0.001$ (GaAs in compression).